JOURNAL OF CATALYSIS 101, 28–34 (1986)

The Leaching-Activation Process of Urushibara Catalysts

ISAAC JACOB,*,[1] MOSHE FISHER,* ZEEV HADARI,*,[1] MORDECHAY HERSKOWITZ,†,[1] JAIME WISNIAK,†,[1] NOAH SHAMIR,‡ AND MOSHE H. MINTZ‡,[2]

*Department of Nuclear Engineering and †Department of Chemical Engineering, Ben-Gurion University of the Negev, P.O. Box 653, Beer-Sheva, Israel; and ‡The Nuclear Research Centre-Negev, P.O. Box 9001, Beer-Sheva, Israel

Received March 19, 1985; revised September 26, 1985

The acid-leaching process resulting in the activation of Urushibara-Ni catalysts was studied by means of X-ray photoelectron spectroscopy (XPS), X-ray diffraction, scanning electron microscopy (SEM) combined with X-ray energy dispersion (EDX), and wet chemical analysis. The leaching-induced activation has been shown to involve the dissolution of a coating surface layer dominated by zinc compounds and the exposure of metallic nickel. Metallic zinc coexisting with the nickel on the activated surface prevents (at low oxidation doses) the oxidation of the inherently active nickel, by gettering the oxidizing molecules. Exposing the active surface to high oxidation doses results in the oxidation of both metallic constituents and the loss of catalytic activity.

INTRODUCTION

Urushibara catalysts (*1*) can be used for the same catalytic reactions as Raney nickel catalysts. Their preparation methods (*2*), however, are much simpler and more convenient than that of Raney nickel. Various modifications of Urushibara catalysts are presently known (*2*). Conventionally, the preparation of these catalysts is carried out in two stages. The first stage involves the deposition of nickel metal by reaction between $NiCl_2$ and a suspension of zinc dust in water. The deposited nickel in the first stage will be termed the "precursor U-Ni" and usually it does not catalyze hydrogenation reactions. The second stage, which results in the activation of the above-mentioned precursor, involves the leaching of the precipitated U-Ni with either a base or an acid. The former activated catalyst is termed as U-Ni-B, whereas the latter is denoted U-Ni-A. Exposing an activated catalyst (either U-Ni-B or U-Ni-A) to the ambient atmosphere results in the loss of its catalytic activity. So far, only one surface analysis study characterizing the precipitated U-Ni precursor has been reported (*3*). The activation mechanism of the leaching treatment has not been studied hitherto by surface analysis methods. From X-ray diffraction studies (*4*) it has been postulated that the activating effect of alkalis or acids consists of exposing the inherently active nickel surfaces of the precipitated nickel by removing an overlayer of zinc hydroxide chloride. No direct observation which confirms this assumption has been reported.

In the present work we have compared the surface characteristics of Urushibara-Ni catalysts before and after the acid leaching treatment. We also investigated the changes occurring on the activated surface upon air exposure. The mechanisms associated with the leaching-activation process and with the air-exposure induced loss of activity are thus elucidated. The roles of nickel and of zinc composing the catalyst are discussed.

EXPERIMENTAL

The precursor U-Ni was prepared by the

[1] Also at the Coal Research Technology Centre, Ben-Gurion University of the Negev, Israel.

[2] Also at the Department of Nuclear Engineering, Ben-Gurion University of the Negev, Israel.

0021-9517/86 $3.00

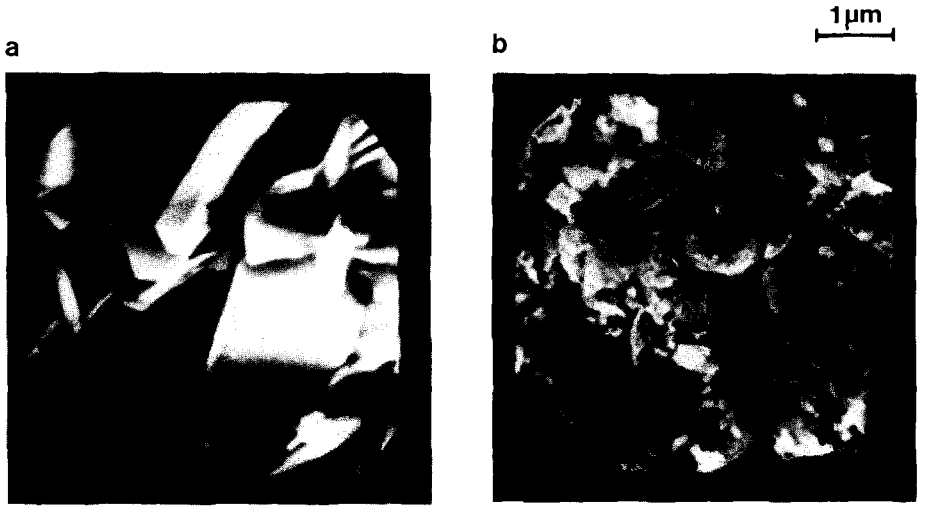

FIG. 1. SEM photographs of the U-Ni precursor (a) and the leached air-exposed U-Ni-A (b) powders.

conventional procedure (*2*) of adding $NiCl_2$ to a suspension of Zn powder in water. Leaching of the U-Ni was conducted by stirring it in 13% acetic acid at room temperature for about 20 min (*2*). The catalytic activity of U-Ni-A was checked by hydrogenating cyclohexanone in a reactor under a hydrogen pressure of 15 atm at 100°C. The identification of the reaction products was performed by gas chromatography. In order to avoid oxidation (which completely obliterates the catalytic activity) of the leached catalyst, it was kept under cyclohexanone. X-Ray photoemission spectra were recorded with the PHI model 549 ESCA/SAM system applying Mg$K\alpha$ radiation (1253.6 eV). The XPS line positions were calibrated according to the Au $4f_{7/2}$ photoelectron peak at 83.8 eV. In cases where charging occurred, the shifted line energies were referenced to the adventitious C 1*s* line at 284.6 eV (*5*). Prior to surface analysis by XPS, the activated catalysts were either air-exposed or handled in argon in a glovebox. The latter sample was utilized in an attempt to simulate as much as possible the activated nonoxidized catalyst used for the catalytic reaction. X-Ray diffraction patterns were obtained for air-exposed samples before and after leaching with a Philips Model PW-1410 diffractometer using Cu$K\alpha$ (λ = 1.5418 Å) radiation. The same samples were examined in a JEOL JSM 35 scanning electron microscope, equipped with facilities for energy dispersive X-ray analysis (EDX). Wet chemical analysis was also performed.

RESULTS

Morphological characterization. Scanning electron microscopy (SEM) photographs of the U-Ni precursor and of the leached (air-exposed) U-Ni-A powders are illustrated in Fig. 1. The U-Ni precursor consists of approximately identical monolithic pieces with hexagonal form of ~1 μm length and thickness of ~0.1 μm. The activated catalyst is characterized by porous peeled-off particles whose maximum dimension does not exceed 0.5 μm.

Surface characterization. The Zn 2*p* photoelectron peaks of the U-Ni precursor, the air-exposed leached U-Ni-A, and the argon-handled leached U-Ni-A are illustrated in Fig. 2 for both the as-inserted samples and for the samples undergoing a short Ar^+ sputtering. For the U-Ni precursor, shifts

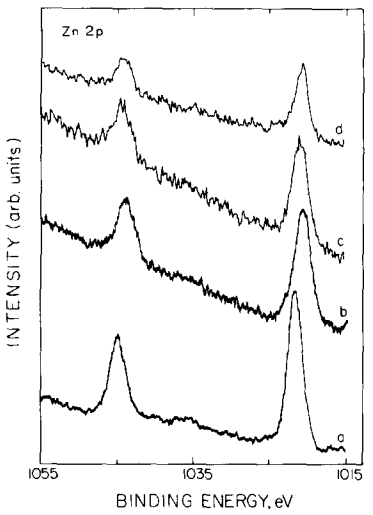

FIG. 2. Zn $2p$ X-ray photoemission spectra from the U-Ni precursor (a), the air-exposed leached U-Ni-A (b), and the argon-handled leached U-Ni-A before (c) and after (d) a short Ar^+ sputtering.

of about 7 eV (toward higher binding energies) occurred in the XPS lines due to charging. These shifts were roughly estimated by referring to the C $1s$ peak and the corrected values are presented in Fig. 2. No charging effects were observed for the leached U-Ni-A samples. The identification of the chemical state of zinc in these samples is much facilitated by referring to the Auger parameter, α, given by the separation between the Zn $2p_{3/2}$ peak and the Zn $L_3M_{45}M_{45}$ Auger line (see Fig. 3). This difference can be accurately determined because static charge corrections cancel. It is customary to present $\alpha + h\nu$ rather than α (where $h\nu$ is the energy of the X-ray photon, which for Mg$K\alpha$ radiation is 1253.6 eV) since this quantity is readily obtained as the sum of the kinetic energy of the Auger electrons and the binding energy of the photoelectron peak. Table 1 lists the $\alpha + h\nu$ values obtained for Zn in the various samples. The existence of two chemical states of Zn on the surface of the argon-handled leached U-Ni-A sample is clearly indicated by these results. The form with $\alpha + h\nu \simeq 2013.5$ eV is attributed to metallic zinc whereas that with $\alpha + h\nu \simeq 2010$ eV is related to some oxidized states (5). Only oxidized states of zinc showed up for the U-Ni precursor and for the air-exposed leached U-Ni-A sample.

The XPS Ni $2p_{3/2}$ lines obtained for the different samples are illustrated in Fig. 4. Actually, no traces of Ni were observed on the U-Ni precursor surface, so only the leached U-Ni-A samples are presented in Fig. 4. The chemical state of the Ni may be deduced from the shapes of the Ni $2p_{3/2}$ lines which display a broad satellite splitting in the case of oxidized Ni, contrary to the sharp-line form of the metallic state. Table 1 lists the different forms of Ni observed on the surfaces of the U-Ni-A specimens. While both metallic and oxidized forms exist on the argon-handled sample only the oxidized state is present on the surface of the air-exposed catalyst.

The O $1s$ photoelectron peaks obtained for the U-Ni precursor as well as for the leached U-Ni-A catalysts displayed a double-peak pattern attributed to oxidic (~530 eV) and hydroxylic (~532 eV) forms. The relative amounts of these forms differed for the different samples.

The existence of chlorine was detected only on the surface of the U-Ni precursor

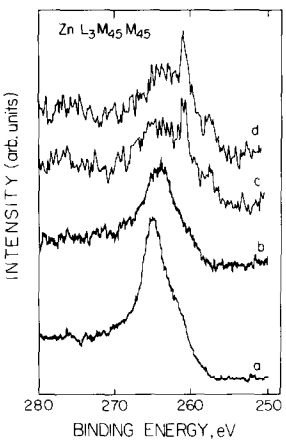

FIG. 3. X-Ray induced Zn $L_3M_{45}M_{45}$ Auger peaks from the U-Ni precursor (a), the air-exposed leached U-Ni-A (b), and the argon-handled leached U-Ni-A before (c) and after (d) a short Ar^+ sputtering.

TABLE 1

Binding Energies (in eV) of Ni, Zn, Cl, and O, the Auger Parameter α of Zn, and the Proposed State of the Zn and the Ni in the Various Samples

Sample	Ni $2p_{3/2}$	Zn $2p_{3/2}$	$\alpha + h\nu^d$	O 1*s*	Cl 2*p*	Proposed states of Zn and Ni
U-Ni	—	1021.2	2009.6	530.3 531.9	198.5	Zn(OH)Cl, ZnO
U-Ni-A[a]	854.1	1021.1	2010.5	529.0 531.0	—	NiO, ZnO
U-Ni-A[b]	852.1 854.5	1021.5	2013.9 2010.8	529.4 531.5	—	Ni, NiO, Zn, ZnO
U-Ni-A[c]	852.3	1020.8	2013.3 2010.1		—	Ni, Zn, ZnO

[a] Air-exposed.
[b] Argon-handled.
[c] Argon-handled after short sputtering.
[d] $h\nu$ = 1253.6 eV.

(by the XPS Cl 2*p* line at 198.5 eV) but not on the surfaces of the leached U-Ni-A.

A quantitative estimation of the relative atomic concentrations of the different surface species was performed by analyzing the Ni 2*p*, Zn $2p_{3/2}$, Cl 2*p*, and O 1*s* peak areas and utilizing the appropriate sensitivity factors (*5*). Table 2 compares these near-surface compositions obtained by XPS (probing depths of about 20–40 Å) to those obtained by EDX (probing depths of a few micrometers) and wet chemical analysis (bulk compositions).

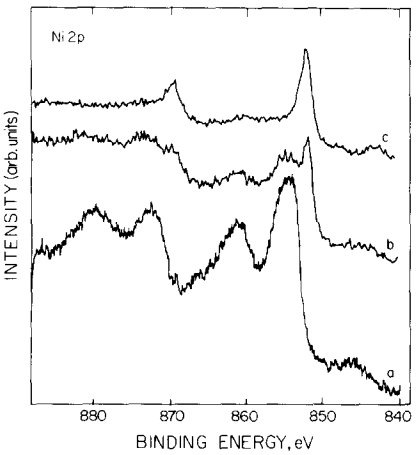

FIG. 4. Ni 2*p* X-ray photoemission spectra from the air-exposed leached U-Ni-A (a) and the argon-handled leached U-Ni-A before (b) and after (c) a short Ar^+ sputtering.

An interesting trend displayed in Table 2 for the U-Ni precursor is the increase in the relative concentration of Ni obtained with increased probing depth of the analytical technique (varying from zero for the surface-sensitive method up to about 0.2 Ni/Zn ratio for the bulk chemical analysis). An opposite trend is displayed for the chlorine and oxygen compositions of that U-Ni sample. These observations point to the existence of a nickel-rich inner core coated by a nickel-depleted (but Cl, O-rich) outer layer in each of the U-Ni powder particles. The absence of any nickel on the outermost surface of the U-Ni as observed in the present study differs to some extent from previous results reported in Ref. (*3*) where some traces of nickel compounds were detected in the zinc-enriched outer layer. From Table 2, the estimated surface O/Zn composition ratio is about 1, the O/Cl ratio is about 2.3, and the Cl/Zn ratio is about 0.4. These results and the existence of hydroxyl groups as indicated in Table 2, suggest that the surface of the U-Ni precursor comprises a possible mixture of Zn(OH)Cl (*2*)

TABLE 2

Relative Atomic Concentrations of the Zn, Ni, Cl, and O Components in U-Ni and U-Ni-A (Air-Exposed) as Determined by XPS, EDX, and Chemical Analysis (CA)

	U-Ni precursor				U-Ni-A (air-exposed)			
	Zn	Ni	Cl	O	Zn	Ni	Cl	O
XPS	100	0	44	102	100[b]	333[b]	0	445
EDX	100	8	28	—[a]	100	1011	0	—
CA	100	20	20	35	100	902	0	986

[a] EDX is not sensitive to oxygen.

[b] The U-Ni-A argon-handled sample exhibits a similar relative atomic concentration of the Ni and Zn components on its surface (from XPS results).

and ZnO with the relative Zn(OH)Cl/ZnO ratio of about 1.

Leaching the U-Ni precursor exposes a nickel-rich surface with a Ni/Zn surface composition ratio of about 3.3. As mentioned above, both metallic surface constituents of the leached catalyst are partially oxidized even for the argon-handled sample. Only an *in situ* Ar^+ sputter-etching produces a metallic nonoxidized surface. Exposing such a metallic surface to 100 Langmuirs of oxygen (1 Langmuir = 10^{-6} Torr · s) results in the partial oxidation of both the zinc and the nickel whereas exposure to the same amount of hydrogen causes partial oxidation (due to the presence of oxidizing impurities in the hydrogen stream) of only the zinc, leaving the nickel in its metallic state.

X-Ray diffraction. The X-ray diffraction patterns of the U-Ni precursor and of the leached (air-exposed) U-Ni-A are presented in Fig. 5. The identification of the various peaks is denoted in the figure. The absence of any lines of either metallic or oxidized nickel in the X-ray pattern of the U-Ni precursor is clearly demonstrated in Fig. 5. The dominant compound identified in that sample is $Zn_5(OH)_8Cl_2$ (*6*), with some traces of metallic zinc and of ZnO. On the other hand, the leached (air-exposed) U-Ni-A is dominated by metallic nickel and NiO with some very weak lines which may be attributed to ZnO. No metallic zinc is indicated in the X-ray diffraction pattern of the leached sample.

Linewidth analysis (*7*) of the diffraction peaks associated with the Ni(111) and the NiO(012) reflections in the leached U-Ni-A yields the mean thicknesses of these crystallites (in the directions normal to the respective planes) to be about 260 and 180 Å, respectively.

DISCUSSION

The lack of catalytic activity displayed by the U-Ni precursor may be attributed to the coating surface layer which is composed of zinc-dominated compounds. The charging effects observed in the XPS of that sample indicate a relatively thick insulating layer coating the powder particles. As indicated by the X-ray diffraction the most dominant compound composing that overlayer is $Zn_5(OH)_8Cl_2$. However, the outermost surface is probably dominated by Zn(OH)Cl and ZnO as concluded from the XPS results. Actually, ZnO is an effective hydrogenation catalyst (*8*) and its presence on the surface should not result in such a pronounced deactivation as displayed by the U-Ni precursor. The observed oxidic zinc is thus probably buried a few monolayers below the topmost layer (composed

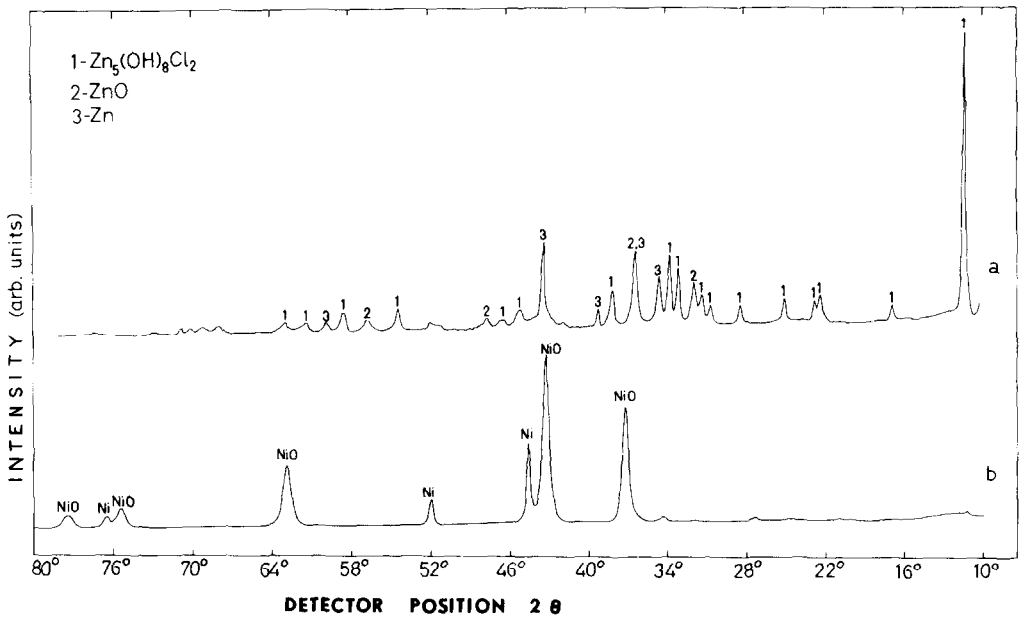

FIG. 5. X-Ray diffraction patterns of the U-Ni precursor (a) and of the leached air-exposed U-Ni-A catalyst (b).

mainly of Zn(OH)Cl) and is thus not involved in the hydrogen–surface interactions. The absence of any nickel lines in the X-ray pattern of the U-Ni may be argued to arise from the substantial thickness of the nickel-depleted insulating overlayer which hinders the presence of a metallic nickel-rich inner core. However, as illustrated by Fig. 1, the U-Ni platelet-like particles have the average dimensions of about 0.1 × 1 × 1 μm which are within the probing depth of the X-ray radiation. The significant concentration of Ni (about 0.2 Ni/Zn ratio as indicated by bulk chemical analysis, cf. Table 2) should thus be detected by X-ray measurements if that nickel were present in its crystalline form (even when buried inside the particles). In addition, no diffraction lines of any Ni–Zn intermetallics or of $Ni(OH)_xCl_y$ compounds were observed. It is thus concluded that the nickel dominating the inner core of the U-Ni particles is precipitated in an amorphous-like form.

Leaching the U-Ni precursor dissolves the zinc-dominated coating layer and exposes the active nickel-rich metallic core. It is well known that metallic nickel is very effective in chemisorbing hydrogen dissociatively (*9*) thereby acting as an efficient hydrogenation catalyst. It is worthwhile to point out the change in the structural form of the nickel induced by the leaching process, which is clearly indicated by the Ni reflections displayed in the X-ray diffraction pattern of the U-Ni-A sample (Fig. 5).

Comparing the XPS-derived Ni/Zn surface composition ratio of the U-Ni-A catalyst to its bulk value (obtained by EDX or CA, Table 2) indicates that the surface of that sample is more enriched with Zn than the bulk. Surface segregation effects of zinc are likely to occur in a Ni–Zn solid solution either due to the characteristics of the melting curve in the corresponding phase diagram (*10*) as suggested by Burton and Machlin (*11*) or due to the lower surface energy of zinc (1020 mJ m^{-2}) as compared with that of nickel (2450 mJ m^{-2}) (*9, 12, 13*). In the oxidized (air-exposed) surface an additional driving force exists, namely the preferred affinity of zinc toward oxygen

which may lead to oxygen-enhanced surface segregation (*9*).

CONCLUSIONS

1. The precipitated U-Ni precursor is composed of particles consisting of an inner metallic core coated by an insulating zinc-dominated layer in agreement with a previous observation (*3*).

2. The outermost surface of the insulating coating layer is composed of ZnO and Zn(OH)Cl which is inactive toward hydrogen chemisorption.

3. Acid leaching of the precipitated precursor dissolves the coating insulating layer exposing the metallic core.

4. The oxidation protection provided by zinc is limited to low oxidation doses. At high oxidation doses surface nickel is oxidized resulting in the loss of the catalytic activity.

REFERENCES

1. Urushibara, Y., *Bull. Chem. Soc. Japan* **25,** 280 (1952).
2. Hata, K., "New Hydrogenating Catalysts: Urushibara Catalysts." Wiley, New York, 1971.
3. Klein, J. C., and Hercules, D. M., *J. Catal.* **82,** 424 (1983).
4. Urushibara, Y., Kobayashi, M., Nishimura, S., and Uehara, H., *Shokubai* **12,** 107 (1956).
5. Wagner, D. C., Riggs, W. M., Davis, L. E., Moulder, J. F., and Muilenberg, G. E., "Handbook of XPS." Physical Electronics, Eden Prairie, Minn. 1979.
6. De Wolff, Techn. Phys. Dienst., Delft, Holland, cited in Powder Diffraction File, Joint Committee on Powder Diffraction Standards, Philadelphia 1967, No. 7-155.
7. Alexander, L., and Klug, H. P., *J. Appl. Phys.* **21,** 126 (1950); Klug, H. P., and Alexander, L., "X-Ray Diffraction Procedure." Wiley, New York, 1951.
8. Dent, A. L., and Kokes, R. J., *J. Phys. Chem.* **73,** 3772 (1969).
9. Schlapbach, L., Seiler, A., Stucki, F., and Siegman, H. C., *J. Less-Common Met.* **73,** 145 (1980).
10. Hansen, M., and Anderko, K., "Constitution of Binary Alloys," p. 1060. McGraw–Hill, New York, 1958.
11. Burton, J. J., and Machlin, E. S., *Phys. Rev. Lett.* **37,** 1433 (1976).
12. Miedema, A. R., *Z. Metallkd.* **69,** 455 (1978).
13. Jacob, I., Fisher, M., and Hadari, Z., *Solid State Commun.* **49,** 1161 (1984).